

## **Supplementary Material:**

### **Ultrafast Detection of Arsenic using Carbon-Fiber Microelectrodes and Fast-Scan Cyclic Voltammetry**

**Noel Manring<sup>1</sup>, Miriam Strini<sup>1</sup>, Jonathan Xavier, Jessica L. Smeltz<sup>1</sup>, Pavithra Pathirathna<sup>1\*</sup>**

**<sup>1</sup>Department of Chemistry and Chemical Engineering, Florida Institute of Technology, 150 W. University Blvd, Melbourne, FL, 32901, USA.**

**\*Correspondence: ppathirathna@fit.edu**

#### **Table of Contents:**

1. Detection of As<sup>3+</sup> in 0.1 M KCl
2. Optimization of scan rate in acidic and basic conditions
3. Stability test in acidic conditions
4. Comparison of As<sup>3+</sup> response on bare CFM and gold nanoparticle-modified CFM
5. Oscilloscope images of the double-bore CFMs in As<sup>3+</sup>-Cd<sup>2+</sup> and As<sup>3+</sup>-Cu<sup>2+</sup> solutions

**Detection of As<sup>3+</sup> in 0.1 M KCl:** We initiated our optimization studies in a simple KCl solution as this is the first time fast-scan cyclic voltammetry (FSCV) has been used with carbon-fiber microelectrodes (CFMs) to detect As<sup>3+</sup> at ultra-fast temporal resolution. As illustrated in Figure S1, we observed an identifiable oxidation peak on the forward scan and a reduction peak on the backward scan for 10 μM As<sup>3+</sup> when scanning from -0.6 V to 1.3 V with a resting potential of -0.6 V in 0.1 M KCl.

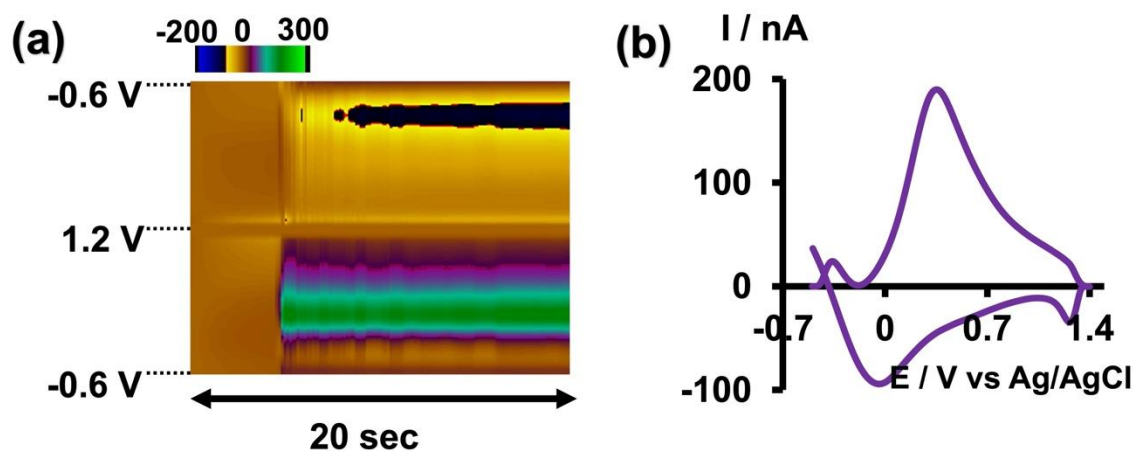


**Figure S1.** Representative (a) color plot and (b) CV for 10 μM As<sup>3+</sup> in 0.1 M KCl.

**Optimization of scan rate in acidic and basic conditions:** After optimizing the positive, negative, and resting potentials, we explored various scan rates from 100 V/s to 500 V/s to identify the optimal scan rate for generating the maximum oxidation/reduction currents and a non-distorted  $\text{As}^{3+}$  CV for both acidic and basic tris solutions. As depicted in Figure S2, the oxidation current for  $\text{As}^{3+}$  in both conditions increased up to 400 V/s, plateauing at 500 V/s. Although the current at 500 V/s was similar to that at 400 V/s, the CV shape appeared distorted; therefore, 400 V/s was chosen as the optimal scan rate.

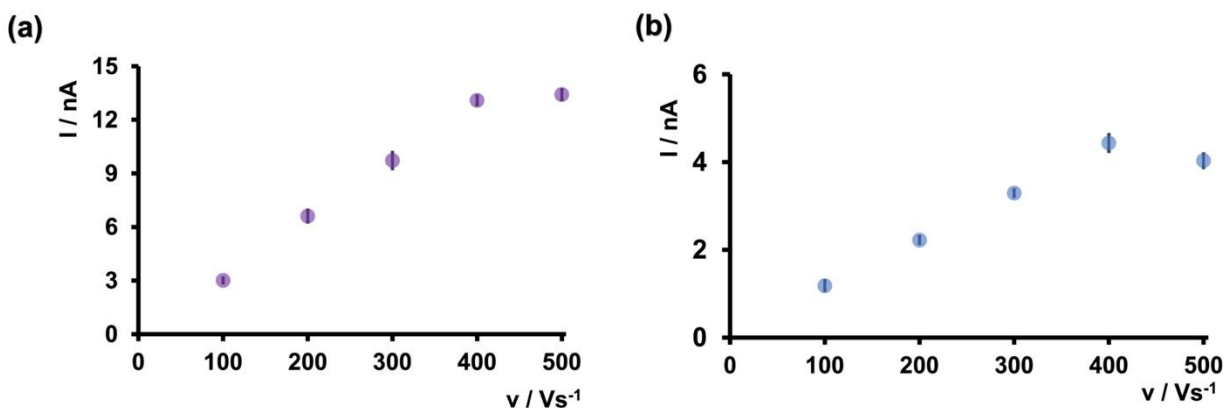


**Figure S2.** (a) The plot of maximum oxidation current vs. scan rate for 5  $\mu\text{M}$   $\text{As}^{3+}$  in tris buffer pH 6.5 upon cycling the potential was from -0.4 V to 1.2 V and back to -0.4 V. (b) The plot of maximum reduction current vs. scan rate for 5  $\mu\text{M}$   $\text{As}^{3+}$  in tris buffer pH 8.5 upon cycling the potential was from 0.5 V to -0.7 V and back to 0.5 V. Each data point represents the average reduction current  $\pm$  standard error of mean obtained for three CFMs with at least four replicate measurements for each CFM (minimum of 12 total replicates).

**Stability test in acidic conditions:** We assessed the sensitivity of our sensor by consecutively injecting  $\text{As}^{3+}$ . As depicted in Figure S3, after 20 consecutive injections of  $1 \mu\text{M}$   $\text{As}^{3+}$ , the maximum oxidation current remained stable, indicating the excellent stability of our sensor.

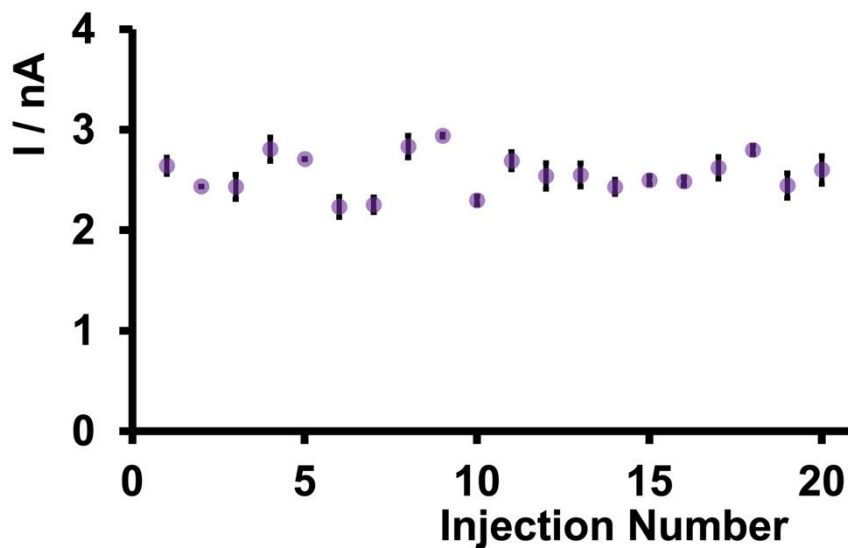


**Figure S3.** Maximum FSCV oxidation current obtained upon successive injections of  $1 \mu\text{M}$   $\text{As}^{3+}$  onto CFMs in tris buffer at pH 6.5. Each data point represents the average oxidation current  $\pm$  standard error of the mean obtained for three CFMs.

**Comparison of  $\text{As}^{3+}$  response on bare CFM and gold nanoparticle-modified CFM:** To enhance the sensing capability of our sensor, we modified CFMs by electrodepositing gold nanoparticles. However, as shown in Figure S4, there was no increase in the oxidation current of  $\text{As}^{3+}$  CV; instead, the response decreased. Therefore, we did not perform further experiments with surface-modified CFMs.

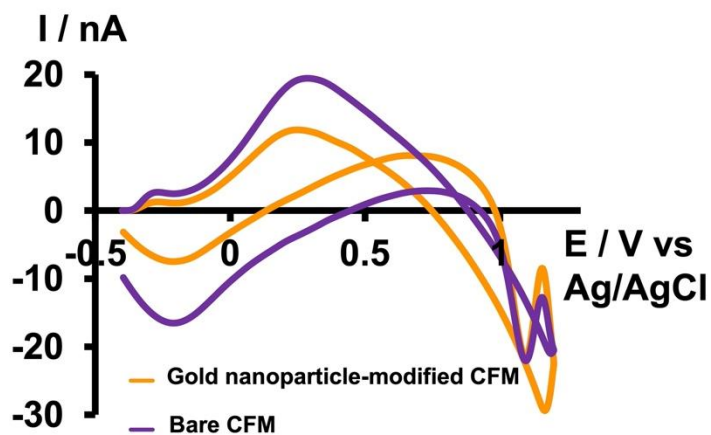


**Figure S4.** (a) Representative CVs obtained for  $10 \mu\text{M As}^{3+}$  with gold nanoparticle-modified CFM (orange) and  $10 \mu\text{M As}^{3+}$  with bare CFM (purple) using acidic waveform in tris buffer pH 6.5.

**Oscilloscope images of the double-bore CFMs in  $\text{As}^{3+}\text{-Cd}^{2+}$  and  $\text{As}^{3+}\text{-Cu}^{2+}$  solutions:** Before conducting co-detection of  $\text{As}^{3+}$  with  $\text{Cd}^{2+}$  and  $\text{Cu}^{2+}$  using double-bore CFMs, we confirmed the stability of the CFMs and tested whether they could maintain a stable gap between the two electrodes. Additionally, we modified one of the CFMs with gold nanoparticles to enable  $\text{Cd}^{2+}$  detection. As shown below, both double-bore CFM assemblies maintained the gap when different potential windows were applied.

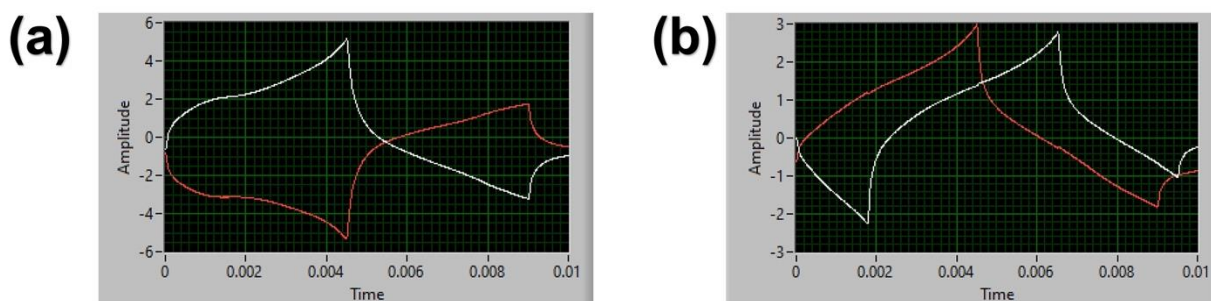


**Figure S5.** Oscilloscope images when two separate waveforms applied to double-bore CFMs in  $\text{As}^{3+}\text{-Cd}^{2+}$  and  $\text{As}^{3+}\text{-Cu}^{2+}$  solutions prepared in tris buffer at pH 6.5. (a) Red line corresponds to the  $\text{Cd}^{2+}$  waveform ( $-0.8\text{ V}$  to  $-1.4\text{ V}$  at  $400\text{ V/s}$ ) and the white line to the  $\text{As}^{3+}$  waveform ( $-0.4\text{ V}$  to  $+1.2\text{ V}$  at  $400\text{ V/s}$ ). (b) Red line corresponds to  $\text{As}^{3+}$  waveform ( $-0.4\text{ V}$  to  $+1.2\text{ V}$  at  $400\text{ V/s}$ ) and the white line corresponds to  $\text{Cu}^{2+}$  waveform ( $-0.7\text{ V}$  to  $+1.2\text{ V}$  at  $400\text{ V/s}$ ).